



The University of
Nottingham

UNITED KINGDOM • CHINA • MALAYSIA

Madan, Christopher R. and Kensinger, Elizabeth A.
(2017) Age-related differences in the structural
complexity of subcortical and ventricular structures.
Neurobiology of Aging, 50 . pp. 87-95. ISSN 1558-1497

Access from the University of Nottingham repository:

http://eprints.nottingham.ac.uk/49069/1/20161018b_draft_clean.pdf

Copyright and reuse:

The Nottingham ePrints service makes this work by researchers of the University of Nottingham available open access under the following conditions.

This article is made available under the Creative Commons Attribution Non-commercial No Derivatives licence and may be reused according to the conditions of the licence. For more details see: <http://creativecommons.org/licenses/by-nc-nd/2.5/>

A note on versions:

The version presented here may differ from the published version or from the version of record. If you wish to cite this item you are advised to consult the publisher's version. Please see the repository url above for details on accessing the published version and note that access may require a subscription.

For more information, please contact eprints@nottingham.ac.uk

1
2
3
4
5
6
7
8
9
10
11
12
13
14
15
16
17
18
19
20
21
22
23
24
25
26

Running head: Complexity of subcortical structures

**Age-related differences in the structural complexity
of subcortical and ventricular structures**

Christopher R. Madan[†] & Elizabeth A. Kensinger
Department of Psychology, Boston College

[†] Corresponding author.

Email address: madanc@bc.edu

Boston College, Department of Psychology,

McGuinn 300, 140 Commonwealth Ave.,

Chestnut Hill, MA, USA 02467

27

Abstract

28 It has been well established that the volume of several subcortical structures decreases in relation
29 to age. Different metrics of cortical structure (e.g., volume, thickness, surface area, gyrification)
30 have been shown to index distinct characteristics of inter-individual differences; thus, it is
31 important to consider the relation of age to multiple structural measures. Here we compare age-
32 related differences in subcortical and ventricular volume to those differences revealed with a
33 measure of structural complexity, quantified as fractal dimensionality. Across three large
34 datasets, totalling nearly 900 individuals across the adult lifespan (18-94 years old), we found
35 greater age-related differences in complexity than volume for the subcortical structures,
36 particularly in the caudate and thalamus. The structural complexity of ventricular structures was
37 not more strongly related to age than volume. These results demonstrate that considering shape-
38 related characteristics improves sensitivity to detect age-related differences in subcortical
39 structures.

40

Keywords:

42 brain morphometry; age; atrophy; fractal dimensionality; thalamus; hippocampus; putamen;
43 ventricles

44

45

Acknowledgements

47 Portions of this research were supported by a grant from the National Institutes of Health
48 (MH080833; to EAK), a fellowship from the Canadian Institutes of Health Research (FRN-
49 146793; to CRM), and by funding provided by Boston College.

50 MRI data used in the preparation of this article were obtained from: (1) the Open Access
51 Series of Imaging Studies (Marcus et al., 2007); (2) the Information eXtraction from Images
52 (IXI) dataset (funded by Engineering and Physical Sciences Research Council [EPSRC] of the
53 UK [EPSRC GR/S21533/02]); and (3) the BC data was acquired with the support of funding
54 from the Searle Foundation, the McKnight Foundation, and the National Institutes of Mental
55 Health.

56 1. Introduction

57 The structure of the brain changes with age, and these changes can be measured in vivo using
58 magnetic resonance imaging (MRI) (Creasey & Rapoport, 1985; Drayer, 1988; Kemper, 1994;
59 Raz & Rodrigue, 2006). While age-related differences are apparent throughout the brain,
60 differences are particularly evident in the volume of subcortical structures (Allen et al., 2005;
61 Goodro et al., 2012; Greenberg et al., 2008; Gunning-Dixon et al., 1998; Inano et al., 2013;
62 Jernigan et al., 2001; Long et al., 2012; Potvin et al., 2016; Raz et al., 2004, 2005; Tamnes et al.,
63 2013; Walhovd et al., 2005, 2011; Yang et al., 2016). Accompanying these changes, the
64 ventricles also enlarge with age (Apostolova et al., 2012; Barron et al., 1976; Kaye et al., 1992;
65 LeMay, 1984; Walhovd et al., 2011; Nestor et al., 2008). Here we investigated age-related
66 changes in the *shape* of these same subcortical structures and tested if this additional information
67 could explain variance beyond that explained by volumetric changes.

68 Walhovd et al. (2011) conducted a comprehensive review of the literature examining age-
69 related differences in subcortical structures. In their review, along with their own multi-sample
70 analyses, they found strong age-related differences in the volume of the putamen, thalamus, and
71 accumbens; other regions, including the caudate and amygdala, were relatively unaffected by
72 aging. Walhovd et al. also found volumetric differences in the lateral ventricles and third
73 ventricle to also be strongly related to age, but no age-related differences in the fourth ventricle.
74 In a supplemental figure (Walhovd et al., 2011, Figure S2), the authors additionally illustrated
75 age differences in the shape of these subcortical structures, though there was no accompanying
76 quantitative analysis of shape.

77 While it is known that there are age-related differences in cortical thickness and
78 gyrification (Hogstrom et al., 2013; Fjell et al., 2009; McKay et al., 2014; Salat et al., 2004),
79 many other morphological measures can also be examined (e.g., sulcal depth, span, and
80 variability [Kochunov et al., 2008; Im et al., 2006; Thompson et al., 1996; Yun et al., 2013];

81 curvature [Fischl et al., 1999; Pienaar et al., 2008]). Recently we demonstrated that age-related
82 differences in the shape, i.e., structural complexity, of cortical regions were more pronounced
83 than in cortical thickness or gyrification (Madan & Kensinger, 2016). Moreover, we found that
84 complexity statistically accounted for all of the age-related differences associated with cortical
85 thickness and gyrification. Although it is currently unclear what features of brain morphology are
86 captured by this metric of complexity, the results underscore that—at least for cortical regions—
87 complexity is a particularly robust metric for assessing age-associated differences. Of course,
88 explaining the ‘most’ age-related variability is not always desired, as this may leave less
89 remaining variance to account for other sources of inter-individual variability (e.g., cognitive
90 abilities); but the extant research suggests that if the goal is to estimate effects of age on brain
91 morphology, metrics of structural complexity may be of particular utility.

92 Here we sought to extend this research by assessing the extent by which complexity can
93 improve the characterization of age-related differences in brain structure beyond the cortex, by
94 examining subcortical and ventricular structures. A number of studies have demonstrated that the
95 shape of subcortical structures can differ between patients and healthy controls. For instance,
96 autism has been associated with differences in the shape of the amygdala (Chung et al., 2008),
97 Alzheimer’s disease has been related to differences in several structures, particularly the
98 hippocampus, amygdala, and lateral ventricles (Tang et al., 2014), and schizophrenic patients
99 have shown differences in hippocampal and thalamus shape (Zhao et al., 2016; also see Smith et
100 al., 2011, and Qiu et al., 2009). Though these studies provide evidence that shape characteristics
101 can be a relevant measure for subcortical structures, it is possible that these systematic
102 differences only occur in the presence of neurological or psychiatric disorders. Furthermore,
103 increased explained variance may not always be desired, instead, we propose that the use of
104 multiple metrics can lead to better characterization of inter-individual differences.

105 Here we used fractal dimensionality to measure the structural complexity of the
106 investigated subcortical and ventricular structures. This approach was inspired by the innovative
107 work of Mandelbrot (1967), where fractal geometry principles were applied to quantify the
108 complexity of complex natural structures. While Mandelbrot initially applied fractal
109 dimensionality to geographic data (coast lines), neuroimagers have previously considered the
110 notion of using fractal dimensionality to quantify the complexity of the brain (e.g., Free et al.,
111 1996; Kiselev et al., 2003). More broadly, fractal dimensionality have been used in neuroscience
112 from the scale of individual neurons to the whole brain (see Di Ieva et al., 2014, 2015, for a
113 review).

114 Using three large datasets, here we first replicated the age-related differences in volume
115 of subcortical and ventricular structures, then further calculated age-related differences in their
116 structural complexity. The present study addressed two primary questions: (1) are there
117 systematic age-related differences in the shape of subcortical structures, as indexed by structural
118 complexity, using the same approach as in Madan and Kensinger (2016) and (2) how do these
119 differences compare to volumetric age-related differences in these structures. Different structural
120 measures may also serve complimentary roles—where different measures may index distinct
121 population-level characteristics; as such we additionally assessed the collinearity of the measures
122 and the unique variance they can explain with respect to age-related variability.

123

124 **2. Procedure**

125 *2.1. Datasets*

126 Three datasets were used to evaluate age-related differences in subcortical and ventricular
127 structure.

128 **Sample 1 (OASIS)** consisted of 314 healthy adults (196 females), aged 18-94, from the publicly
129 available Open Access Series of Imaging Studies (OASIS) cross-sectional dataset (Marcus et al.,

130 2007; <http://www.oasis-brains.org>). Participants were recruited from a database of individuals
131 who had (a) previously participated in MRI studies at Washington University, (b) were part of
132 the Washington University Community, or (c) were from the longitudinal pool of the Washington
133 University Alzheimer Disease Research Center. Participants were screened for neurological and
134 psychiatric issues; the Mini-Mental State Examination (MMSE) and Clinical Dementia Rating
135 (CDR) were administered to participants aged 60 and older. In the current sample, participants
136 with a CDR above zero were excluded; all remaining participants scored 25 or above on the
137 MMSE. Multiple T₁ volumes were acquired using a Siemens Vision 1.5 T with a MPRAGE
138 sequence; only the first volume was used here. Scan parameters were: TR=9.7 ms; TE=4.0 ms;
139 flip angle=10°; voxel size=1.25×1×1 mm.

140 **Sample 2 (IXI)** consisted of 427 healthy adults (260 females), aged 20-86, from the publicly
141 available Information eXtraction from Images (IXI) dataset ([http://brain-development.org/ixi-](http://brain-development.org/ixi-dataset/)
142 [dataset/](http://brain-development.org/ixi-dataset/)). This is the same set of individuals we used previously to investigate age-related
143 differences in the cortex (Madan & Kensinger, 2016). These individuals were scanned at one of
144 three hospitals in the London, UK (Guy's Hospital, Hammersmith Hospital, and Institute of
145 Psychiatry) in 2005-2006. Details on how these individuals were recruited is unavailable, nor are
146 details on how mental health was assessed. See Madan and Kensinger (2016) for further details.

147 **Sample 3 (BC)** consisted of 176 healthy adults (89 females), aged 18-83, recruited by the
148 Cognitive and Affective Laboratory at Boston College (BC) in 2012-2015. All participants were
149 screened for neurological and psychiatric issues, and to have scored above 26 on the MMSE. T₁
150 volumes were acquired using a Siemens Trio 3 T with a MEMPRAGE sequence optimized for
151 morphometry studies (van der Kouwe et al., 2008; Wonderluck et al., 2009). Scan parameters
152 were: TR=2530 ms; TE=1.64, 3.50, 5.36, 7.22 ms; flip angle=7°; voxel size=1×1×1 mm.

153 *2.2. Segmentation and volumetric analyses*

154 All structural MRIs were processed using FreeSurfer 5.3.0 on a machine running CentOS 6.6
155 (Fischl, 2012; Fischl & Dale, 2000; Fischl et al., 2002). FreeSurfer's standard pipeline was used
156 (i.e., `recon-all`). FreeSurfer's segmentation procedure produces labels for seven subcortical
157 structures (thalamus, hippocampus, amygdala, caudate, putamen, accumbens, palladium) and
158 four ventricular structures (lateral, inferior lateral, third, fourth) all within a common
159 segmentation volume (Fischl et al., 2002, 2004). Figure 1 shows the subcortical structures
160 investigated here. Volumes for subcortical and ventricular structures were obtained directly from
161 FreeSurfer.

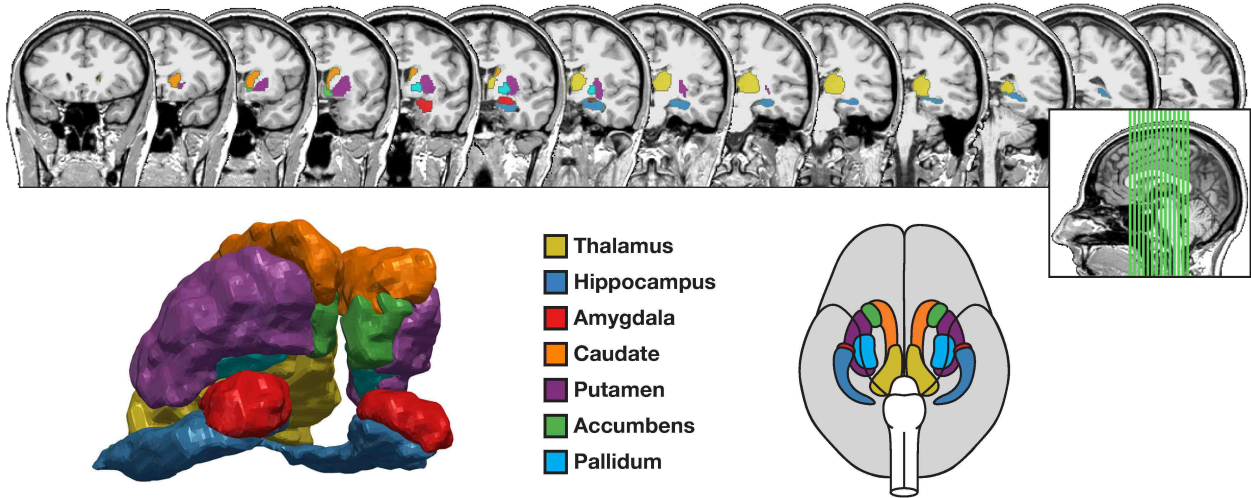
162 Validation studies have shown that this automated segmentation procedure corresponds
163 well with manual tracing (e.g., Fischl et al., 2002; Jovicich et al., 2009; Keller et al., 2012;
164 Lehmann et al., 2010; Mulder et al., 2014; Pardoe et al., 2009; Tae et al., 2008; Wenger et al.,
165 2014). FreeSurfer has been used in a large number of studies investigating age-differences in
166 subcortical structures (e.g., Inano et al., 2013; Jovicich et al., 2009; Long et al., 2012; Potvin et
167 al., 2016; Tamnes et al., 2013; Walhovd et al., 2005, 2011; Wenger et al., 2014; Yang et al.,
168 2016).

169 Intracranial volume (ICV) was also estimated using FreeSurfer (Buckner et al., 2004),
170 which has also been shown to correspond well with manual tracing (Sargolzaei et al., 2015).

171

172

173



174
 175 **Figure 1. Coronal slices, 3D reconstruction, and 2D illustration of the seven subcortical**
 176 **structures examined.** Coronal slices, with anterior slices on the left, are shown at 5-mm spacing
 177 from a representative participant; positions of the displayed coronal slices are marked on the
 178 inset sagittal slice. The 3D reconstruction is based on the same participant’s MRI as the coronal
 179 slices (following from Madan, 2015). The 2D illustration was adapted from Toro et al. (2014).
 180

181 2.3 Fractal dimensionality analyses

182 The complexity of each structure was calculated using the calcFD toolbox (Madan & Kensinger,
 183 2016; <http://cmadan.github.io/calcFD/>). This toolbox calculates the ‘fractal dimensionality’ of a
 184 3D structure, and is specifically designed to use intermediate files from the standard FreeSurfer
 185 analysis pipeline, here `aparc.a2009s+aseg.mgz`. The toolbox has previously been used with
 186 parcellated cortical structure, as well as validated using several benchmark volumes (Madan &
 187 Kensinger, 2016).

188 We use fractal dimensionality as a measure of the complexity of a 3D structure, i.e., a
 189 subcortical structure. Unlike volume, which corresponds to the ‘size’ of any 3D structure, fractal
 190 dimensionality measures shape information and is scale invariant (Madan & Kensinger, 2016).
 191 In fractal geometry, several approaches have been proposed to quantify the ‘dimensionality’ or
 192 complexity of a fractal; the approach here calculates the Minkowski–Bouligand or Hausdorff
 193 dimension (see Mandelbrot, 1967). This structural property can be measured by considering the
 194 3D structure within a grid space and counting the number of boxes that overlap with the edge of

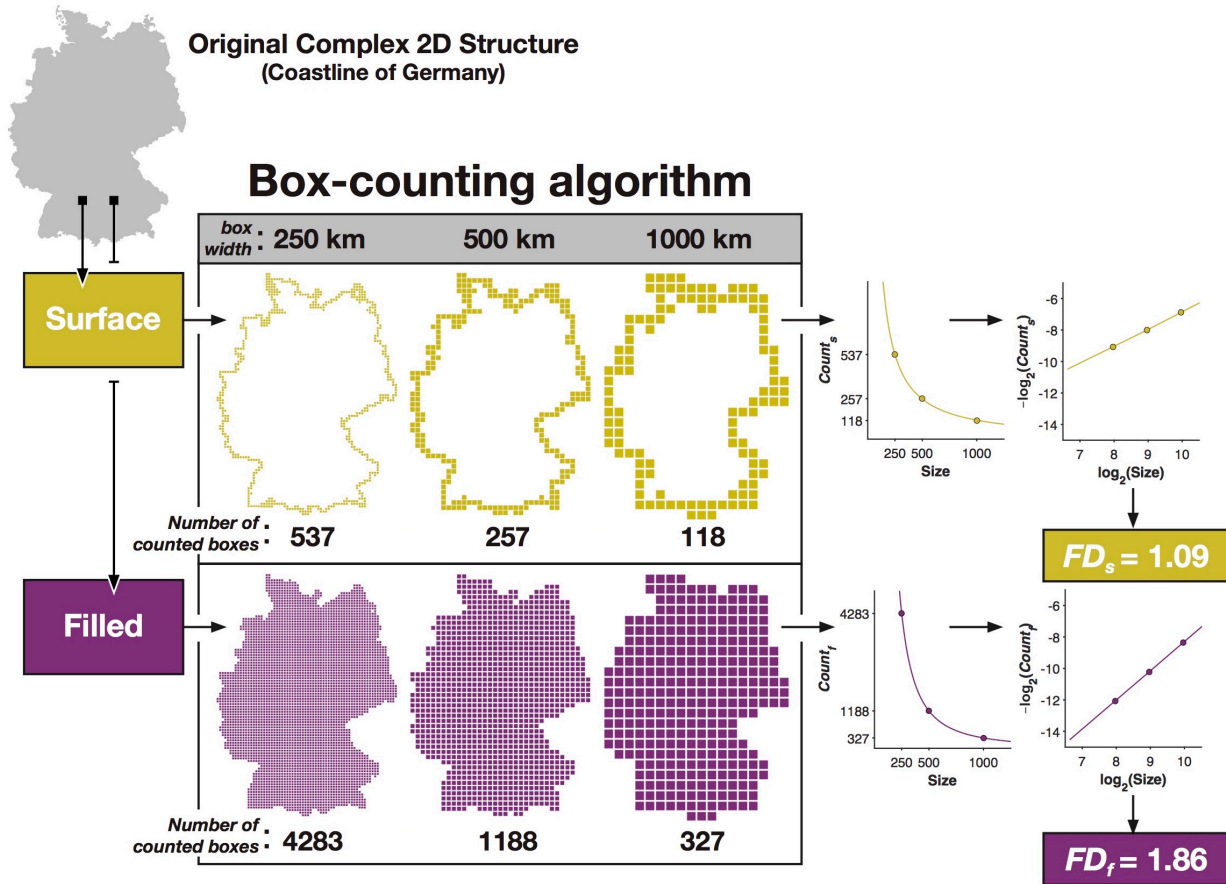
195 the structure, referred to as the ‘box-counting algorithm’ (Caserta et al., 1995; Mandelbrot,
 196 1982). By then using another grid size (i.e., changing the box width), the relationship between
 197 the grid size and number of counted boxes can be determined. Here we used box sizes (in mm)
 198 corresponding to powers of 2, ranging from 0 to 4 (i.e., 2^k [$k = 0, 1, 2, 3, 4$] = 1, 2, 4, 8, 16 mm).
 199 The slope of this relationship in log-log space is the fractal dimensionality of the structure. Thus,
 200 the corresponding equation is:

$$FD = - \frac{\Delta \log_2(\text{Count})}{\Delta \log_2(\text{Size})}$$

201
 202 There are two distinct fractal dimensionality values that can be calculated: If only the boxes
 203 overlapping with the edge/surface of the structure are counted, this slope represents the fractal
 204 dimensionality of the *surface*, denoted as FD_s . If the boxes within the structure are also counted,
 205 the resulting slope represents the fractal dimensionality of the *filled* volume, denoted as FD_f .

206 As the relative alignment of the grid space and the structure can influence the obtained
 207 fractal dimensionality value using the box-counting algorithm, we instead used a dilation
 208 algorithm that is equivalent to using a sliding grid space and calculating the fractal
 209 dimensionality at each alignment (Madan & Kensinger, 2016), but can be calculated much faster
 210 as it is less computationally demanding. This was implemented using a 3D-convolution
 211 operation (convn in MATLAB). As an example, Figure 2 illustrates the calculation of fractal
 212 dimensionality for a complex 2D structure.

213



214

215 **Figure 2. Illustration of how fractal dimensionality is measured from a 2D structure.**

216 Reprinted from Madan and Kensinger (2016) with permission. Copyright 2016, Elsevier.

217

218 *2.4. Data Analysis*

219 All volume measurements were ICV-corrected prior to conducting the regression analyses.

220 Specifically, ICV-corrected volumes were calculated as the residual after the volume data was

221 regressed for ICV (as in Walhovd et al., 2011). Formal comparisons of procedures used to adjust

222 for ICV suggest that results generalize across differing procedures (Greenberg et al., 2008).

223 Age differences in the subcortical and ventricular structures was first assessed using

224 regression models examining the linear and quadratic relationships between age and volume (or

225 fractal dimensionality) of the structure, with the amount of variance explained (i.e., R^2) as the

226 statistic. All of the regression models reported controlled for effects of sex (and site, in the case

227 of the IXI dataset).

228 To directly assess if fractal dimensionality explained more age-related variability than
229 volume, we formally compared model fits based on either measure, for each structure, using the
230 Bayesian Information Criterion (*BIC*). This approach allows us to compare different regression
231 models and determine which model fits the data best, or if models perform comparably.
232 Additionally, models with more parameters are penalized for these additional degrees of
233 freedom. As a rule of thumb, if the difference in *BIC* between two models is less than two,
234 neither of the models' fit to the data is significantly better (Burnham & Anderson, 2002, 2004).
235 As absolute *BIC* values are arbitrary, we subtract the *BIC* value for the best model considered
236 from all *BIC* values and report ΔBIC for each of the models, as is common practice. As a result,
237 the best model considered is $\Delta BIC=0.00$ by definition.

238

239 **3. Results**

240 *3.1. Age-related differences in subcortical structures*

241 We used the OASIS dataset as our primary sample because Walhovd et al. (2011) previously
242 examined age-related differences in volumetric measures in this sample (Samples 4a and 4b in
243 their analyses). As such, the volumetric analyses here were intended to serve as a replication of
244 their findings.

245 The subcortical structures investigated here were the thalamus, hippocampus, amygdala,
246 caudate, putamen, accumbens, and pallidum; a representative reconstruction of the structures
247 from a participant's MRI is shown in Figure 1. As shown in Table 1, linear and quadratic
248 relationships between age and volumes of subcortical structures closely matched the amount of
249 variance explained (i.e., R^2) reported by Walhovd et al. for the same sample. Briefly, age-related
250 differences were most pronounced in the thalamus, putamen, accumbens, and pallidum—each
251 with R^2 values near 50% or above (Figure 3A). Age explained a moderate amount of variability

252 in the volume of the hippocampus and amygdala, whereas caudate volume was the least related
 253 to age-related differences. The upper half of Figure 4 shows the quadratic fits for each structure.

254 We calculated the fractal dimensionality, both FD_s and FD_f , of the structures for each
 255 individual to additionally measure age-related differences in their structural complexity. Fractal
 256 dimensionality of the surface (FD_s) captured more variability than volume for some of the
 257 structures; for instance, 64% for the thalamus and 66% for the accumbens. There was a smaller
 258 increase in variability explained by FD_s relative to volume in the amygdala (31%) and there was
 259 effectively no additional age-related differences explained in the caudate (16%). However, less
 260 variability was explained by FD_s than by volume in other structures, such as the hippocampus
 261 (20%), putamen (31%), and pallidum (36%). Importantly, FD_s captures shape-related, but not
 262 volumetric, characteristics of the surface structure. In contrast, FD_f , while scale invariant, is
 263 influenced by a combination of shape- and volumetric-related characteristics of the structure.
 264 Age-related differences in FD_f were larger than those for volume across all seven subcortical
 265 structures, as shown in Table 1 and Figure 3A; differences were also larger than for FD_s for all
 266 but one structure, though that comparison was only nominally smaller [accumbens, quadratic R^2 :
 267 $FD_s = 66\%$; $FD_f = 65\%$]. Relative to volume, the amount of variability explained in FD_f was
 268 much higher for the thalamus and caudate (74% and 40% variance explained with the quadratic
 269 model, respectively; versus 55% and 12% with volume, respectively). More moderate increases
 270 (of approximately 10% more variance explained) were found for the amygdala, putamen, and
 271 accumbens. The lower half of Figure 4 shows the quadratic fits for the structures; relationships
 272 are generally consistent as those with volume, though generally there is less unexplained
 273 variability (i.e., the residual).

274 Figure 3B illustrates that volume and structural complexity are highly collinear. Volume
 275 and structural complexity were the most distinct for the caudate, with 59% shared variance.
 276 Apart from the caudate, the amount of shared variance ranged from 73-86%. Including both

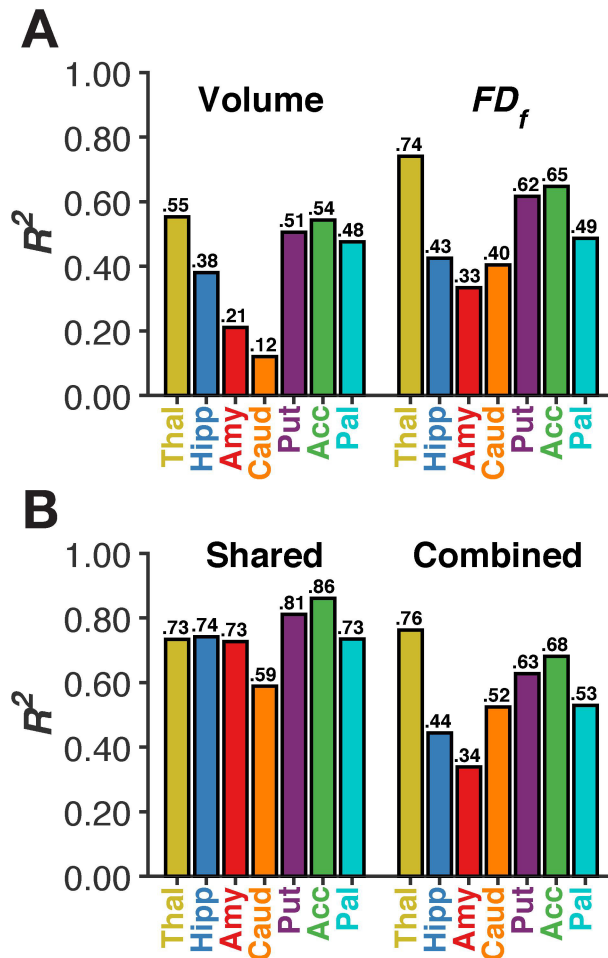
277 volume and structural complexity within the same model marginally increased the total amount
278 of variance explained (Figure 3B) relative to the FD_f models, with increases ranging from 1-4%
279 for six of the structures. However, the inclusion of volume led to a 12% additional variance
280 explained for the caudate, suggesting that age-related differences in volume and complexity were
281 distinct for this region.

282 The two fractal dimensionality measures were slightly more collinear, with shared
283 variances of: thalamus (77%), hippocampus (71%), amygdala (85%), caudate (76%), putamen
284 (63%), accumbens (99%), and pallidum (72%). In almost all cases, the combined variance
285 explained by the two fractal dimensionality measures was increased by less than 5% relative to
286 the FD_f -only regression model; the only exception to this was the caudate, where the combined
287 model explained 56% of age-related variability.

288 Formal model comparisons are reported in Table 2. In contrast to the analyses presented
289 in Figures 3-4 and Table 1, where the structural measures were used as the dependant variable
290 (DV), here we used age as the DV such that we could compare how well the various structural
291 measures were able to explain variability in this common DV. Here we found that fractal
292 dimensionality explained more age-related variability than volume for all of the subcortical
293 structures.

294

295

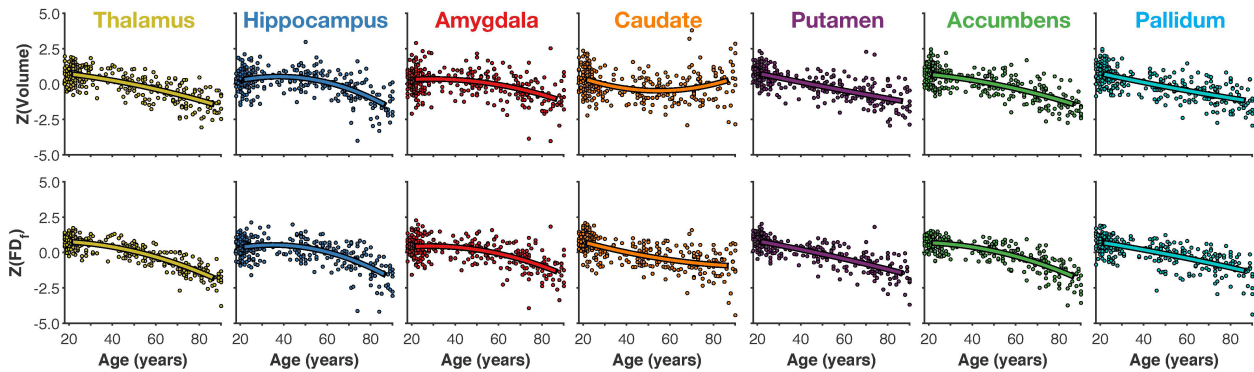


296

297 **Figure 3. Amount of variance explained (R^2) by quadratic models of age in volume and**
 298 **structural complexity for each subcortical structure (Panel A). Panel B shows the amount**
 299 **of variance common to both volume and complexity (i.e., collinearity), as well as combined**
 300 **variance explained by including both volume and complexity.**

301

302



303

304 **Figure 4. Scatter plots of age-related differences in volume and structural complexity for**
 305 **each subcortical structure along with best-fitting quadratic models.**

306

307

	Volume						FD_f					
	1		2		3		1		2		3	
	OASIS		IXI		BC		OASIS		IXI		BC	
	Age	Age ²	Age	Age ²	Age	Age ²	Age	Age ²	Age	Age ²	Age	Age ²
Thalamus	.55	<u>.55</u>	.28	.30	.28	.37	.71	.74	.52	.54	.51	.56
Hippocampus	.26	.38	.14	.20	.38	.47	.31	.43	.10	.13	.26	.32
Amygdala	.18	.21	.10	.12	.35	.42	.28	.33	.23	<u>.24</u>	.42	.48
Caudate	.03	.12	.05	.06	.04	.10	.39	<u>.40</u>	.26	.26	.29	<u>.31</u>
Putamen	.51	.51	.28	.28	.50	<u>.51</u>	.62	.62	.32	.32	.44	.46
Accumbens	.53	.54	.23	.23	.44	.45	.61	.65	.31	.31	.47	<u>.49</u>
Pallidum	.47	.48	.06	.06	.33	.34	.49	.49	.10	.11	.30	.31
<i>Ventricles</i>												
Lateral	.53	.60	.32	.38	.44	.48	.51	.53	.26	.28	.48	.48
Inferior Lateral	.39	.57	.19	.28	.28	.32	.30	.41	.07	.09	.25	<u>.28</u>
3rd	.52	.63	.30	.34	.44	.49	.52	.59	.28	.30	.43	.47
4th	.02	.08	.01	<u>.02</u>	.00	.00	.00	.08	.00	<u>.01</u>	.01	.01

308 **Table 1. Effects of age on volume and fractal dimensionality for the structures examined.**
309 Volume measures were ICV-corrected; effects of site were regressed out for the IXI sample.
310 Values in the Age² columns indicate amount of explained variance (R^2) for the model consisting
311 of Age+Age² and are printed in bold/italic+underline only if the addition of the quadratic term
312 significantly increased the amount of explained variance. **Bold:** $p < .01$; *Italic+Underline:* $p < .05$.

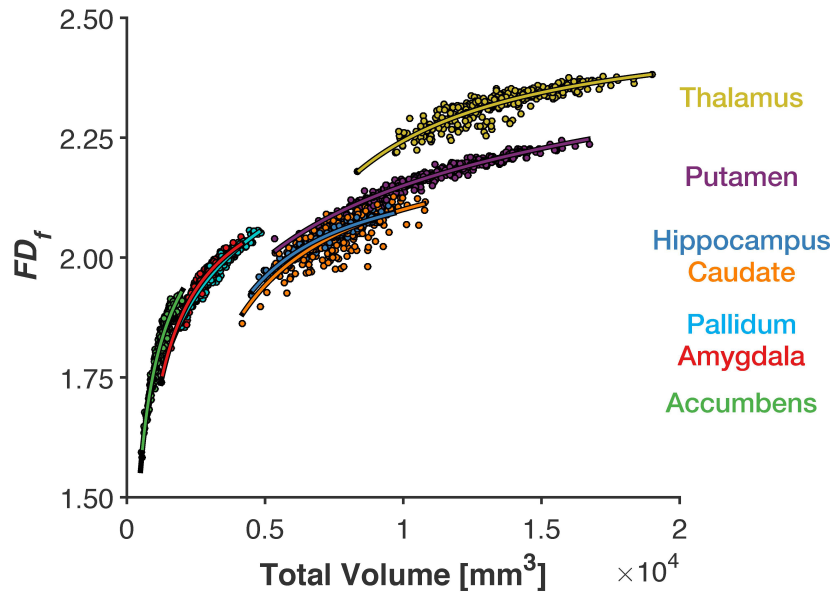
313 *3.2. Limitations to scale invariance of fractal dimensionality*

314 While fractal dimensionality is mathematically scale invariant, constraints of MRI data
315 acquisition may introduce a lower limit to this theoretical property. Specifically, smaller
316 structures are inherently more ‘rectangular’ due to voxel resolution constraints and thus will have
317 lower structural complexity as a result. A lower limit on the scale invariance of fractal
318 dimensionality would appear as a steep relationship with volume, indicating that the resolution of
319 the 3D structure’s shape was insufficient to yield additional contributions from shape-related
320 properties.

321 Here we examined the relationship between total volume (without ICV-correction) and
322 FD_f and found some evidence of a limitation in scale invariance (Figure 5). Specifically, smaller
323 subcortical structures (e.g., accumbens, pallidum) had steeper relationships between volume and
324 FD_f and less ‘off-axis’ variability than larger structures (e.g., thalamus, caudate). This indicates
325 that (1) FD_f for smaller structures was influenced more by volumetric characteristics than in the
326 larger structures, and (2) FD_f for smaller structures was more correlated with volume, while FD_f
327 for larger structures additionally indexed other sources of variability (i.e., shape-related
328 characteristics). This increase in off-axis variability was not true of all larger structures,
329 specifically the putamen, though this could be related to biological constraints in the variability
330 in shape of the structure.

331 These results indicate that future applications of structural complexity will be limited for
332 structures that are inherently small (e.g., hippocampal subfields), though this limitation can be
333 attenuated by acquiring MRI data with higher-resolution imaging protocols (i.e., decreasing the
334 voxel size during acquisition). As noted in the Methods section, the MRI data in the datasets
335 analyzed here were acquired with a voxel size of 1 mm³-isotropic or slightly larger. However,
336 when anatomical fidelity is critical, current neuroimaging protocols can acquire high-resolution

337 images with voxel dimensions on the scale of 0.5 mm in-plane (e.g., Hrybouski et al., 2016; La
338 Joie et al., 2010; Palombo et al., 2013; Reagh & Yassa, 2014; Yushkevich et al. 2015).
339



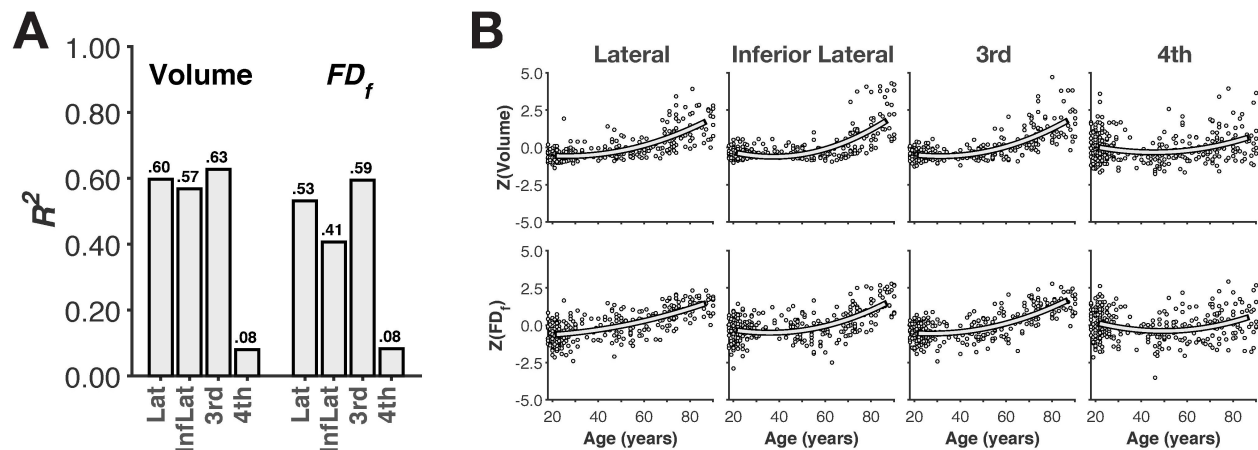
340
341 **Figure 5. Scatter plot of total volume and structural complexity along with best-fitting**
342 **power-function models.**

343 3.3. Age-related differences in the ventricles

344 We also examined age-related differences in the volume and structural complexity of the
 345 ventricles, as shown in Figure 6. The amount of variability in volume explained by age-related
 346 differences was consistent with Walhovd et al. (2011). Interestingly, variability in the fractal
 347 dimensionality (FD_f) of the structures was more weakly associated with age-related differences
 348 than volume, unlike the subcortical structures (see Table 1). When formally compared (see
 349 below), volume explained more age-related variability than fractal dimensionality for all of the
 350 ventricular structures (Table 2).

351

352



353

354 **Figure 6. Age-related differences in volume and structural complexity of ventricular**
 355 **structures.** (A) Bar plot of amount of variance explained (R^2) by quadratic models of age. (B)
 356 Scatter plots of age-related differences in either measure.

357

	Volume		FD_f	
	Linear	Quadratic	Linear	Quadratic
Thalamus	138.81	144.04	0.00	1.97
Hippocampus	294.06	292.48	268.43	274.18
Amygdala	325.39	328.65	282.02	285.23
Caudate	378.02	374.80	230.20	234.18
Putamen	166.08	166.43	87.17	91.08
Accumbens	148.45	146.21	88.52	85.10
Pallidum	185.06	188.54	178.19	177.54
<i>Ventricles</i>				
Lateral	151.21	111.27	160.55	148.52
Inferior Lateral	229.71	212.61	274.11	260.23
3rd	156.98	123.98	154.28	144.76
4th	380.47	385.83	386.21	387.84

358 **Table 2. Model fitness in comparing the effects of volume and fractal dimensionality in**
359 **explaining age, for each of the structures examined, based on the OASIS dataset.** Values in
360 the Quadratic columns indicate model fitness (ΔBIC) for the regression model consisting of both
361 linear and quadratic terms. Models with BIC values with a difference greater than two suggest
362 that the model with the lower BIC value is a significantly better fit than the other models. Best
363 fitting models for each structure are denoted in **bold**.
364

365 3.4. Replication in independent samples

366 To assess the reproducibility of our findings of age-related differences in the structural
367 complexity of the subcortical and ventricular structures, we conducted similar analyses in two
368 additional samples.

369 In the IXI sample, we generally found less age-related differences in both volume and
370 fractal dimensionality; however, the volumetric differences observed here were within the inter-
371 sample variability observed in Walhovd et al. (2011). Importantly, the same regions were found
372 to show the strongest age-related differences in volume (e.g., thalamus, putamen, lateral
373 ventricles; though not the pallidum). Fractal dimensionality (FD_f) was again more closely related
374 to age-related differences. Results in the BC sample were consistent with those observed in the
375 OASIS and IXI samples, and magnitudes of explained variance on age-related differences in
376 volume and fractal dimensionality were generally in-between those observed in each of the other
377 datasets.

378

379 4. Discussion

380 When examining age-related differences in brain structure, it is important to consider the most
381 appropriate measure. With cortical structure, it has been established that age-related differences
382 are reflected most in cortical thickness, rather than surface area or volume (Hogstrom et al.,
383 2013; Fjell et al., 2009; McKay et al., 2014; Salat et al., 2004); however, we recently
384 demonstrated that structural complexity of the cortex is more sensitive to age-related differences
385 than thickness (Madan & Kensinger, 2016). In the present study, we found systematic age-
386 related differences in the structural complexity of subcortical regions that was not captured by
387 volumetric measures. Additionally, we found that structural complexity was not more closely
388 related to age-related differences across all brain structures: this measure showed a weaker
389 association with age for the ventricular regions than did other metrics. Thus, it is clear that

390 considering the shape of subcortical structures provides additional information about age-related
391 atrophy beyond ICV-corrected volume, but only when the ‘contents’ of the structure are
392 themselves meaningful—i.e., neural tissue, rather than CSF.

393 Evidence of age-related differences in fractal dimensionality in subcortical structures (as
394 well as cortical structures; Madan & Kensinger, 2016) demonstrates that current approaches of
395 measuring age-related differences in volume (and cortical thickness) only partially characterize
396 how the structural properties of the brain relate to age. While the neurobiological basis (i.e.,
397 cellular through systems level) of these differences is unclear, these differences are demonstrably
398 evident at the macro-level of brain structures that is measured using structural MRIs. Further
399 research is needed to establish how these shape-related differences manifest in more precise
400 measures of neural structure (e.g., differences in neuronal composition or density). Indeed, the
401 use of fractal dimensionality to measure complexity at the micro- and meso-level structures
402 within neuroscience has already been established (Di Ieva et al., 2014, 2015) and may prove
403 useful in examining age-related differences within these subcortical structures, such as in the
404 composition of neurons. Nonetheless, the present results provide evidence of an additional metric
405 for evaluating inter-individual differences in physiological brain age.

406 Prior work in young and older adults has demonstrated that fractal dimensionality can
407 index inter-individual differences in brain morphology that relate to cognition and differs
408 between healthy adults and patient populations. While the current work applies fractal
409 dimensionality analyses to subcortical structures, others have used fractal dimensionality to
410 characterize the structural complexity of segmented grey or white matter structure (e.g., King et
411 al., 2009; Madan & Kensinger, 2016; Mustafa et al., 2012; Sandu et al., 2008). Using these
412 approaches, fractal dimensionality has been related to inter-individual differences in measures of
413 fluid intelligence (Mustafa et al., 2012; Sandu et al., 2014), IQ (Im et al., 2006), and performance
414 on the cognitive subscale of the Alzheimer’s Disease Assessment Scale (King et al., 2010).

415 Fractal dimensionality has also been shown to differ between healthy adults and a number of
416 patient populations, particularly in Alzheimer's disease (King et al., 2009, 2010; Thompson et
417 al., 1998) and schizophrenia (Ha et al., 2005; Narr et al., 2004; Nenadic et al., 2014; Sandu et al.,
418 2008; Yotter et al., 2011; Zhao et al., 2016). Thus, while we have demonstrated the benefits of
419 using fractal dimensionality to index age-related differences in subcortical structure, as well as
420 cortical structure (Madan & Kensinger, 2016), the variability of this morphological measure also
421 is related to inter-individual differences in cognitive measures and may hold promise as a
422 biomarker for some neurological disorders. However, it is important to consider that more inter-
423 individual variability explained by age may not always be desired, as this leaves less variance
424 available to be related to other factors, e.g., performance on cognitive measures, so volume may
425 still be a preferable measure depending on the research question. As such, we advocate for the
426 use of multiple brain morphology measures when examining inter-individual differences.

427 Though we measured structural complexity here using fractal dimensionality, this is not
428 the only approach to quantify these shape-related properties; other related approaches such as
429 spherical harmonics (Chung et al., 2008, 2010; Yotter et al., 2011) and Laplace-Beltrami spectra
430 (Reuter et al., 2006; Wachinger et al., 2015) may similarly be able to capture these structural
431 differences. Seo and Chung (2011) demonstrated that Laplace-Beltrami eigenfunctions can yield
432 better fits to the original structure than spherical harmonics, when reconstructing cortical and
433 subcortical surfaces. This difference was attributed to Laplace-Beltrami spectra not necessitating
434 spherical parameterization. As of yet, no comparison has been done between Laplace-Beltrami
435 spectra and the current approach of using fractal dimensionality.

436 In summary, the present results reveal that metrics of fractal dimensionality can capture
437 age-associated variance within subcortical structures that is missed when using only volumetric
438 measures. This result represents an important extension of prior research examining cortical
439 structure (Madan & Kensinger, 2016), revealing that fractal dimensionality is strongly associated

440 with age even in relatively small, subcortical structures. Moreover, these results emphasize the
441 benefits of including metrics of fractal dimensionality in assessments of structural differences
442 associated with aging and of assessing both subcortical and cortical structures.

References

- 443
444 Allen, J. S., Bruss, J., Brown, C. K., & Damasio, H. (2005). Normal neuroanatomical variation
445 due to age: The major lobes and a parcellation of the temporal region. *Neurobiology of*
446 *Aging*, *26*, 1245–1260. doi:10.1016/j.neurobiolaging.2005.05.023
- 447 Apostolova, L. G., Green, A. E., Babakchanian, S., Hwang, K. S., Chou, Y.-Y., Toga, A. W., &
448 Thompson, P. M. (2012). Hippocampal Atrophy and Ventricular Enlargement in Normal
449 Aging, Mild Cognitive Impairment (MCI), and Alzheimer Disease. *Alzheimer Disease &*
450 *Associated Disorders*, *26*, 17–27. doi:10.1097/wad.0b013e3182163b62
- 451 Barron, S. A., Jacobs, L., & Kinkel, W. R. (1976). Changes in size of normal lateral ventricles
452 during aging determined by computerized tomography. *Neurology*, *26*, 1011–1011.
453 doi:10.1212/wnl.26.11.1011
- 454 Buckner, R. L., Head, D., Parker, J., Fotenos, A. F., Marcus, D., Morris, J. C., & Snyder, A. Z.
455 (2004). A unified approach for morphometric and functional data analysis in young, old,
456 and demented adults using automated atlas-based head size normalization: Reliability and
457 validation against manual measurement of total intracranial volume. *NeuroImage*, *23*, 724–
458 738. doi:10.1016/j.neuroimage.2004.06.018
- 459 Burnham, K. E., & Anderson, D. R. (2002). *Model selection and multimodel inference (2nd ed.)*.
460 New York: Springer-Verlag.
- 461 Burnham, K. P., & Anderson, D. R. (2004). Multimodel inference: Understanding AIC and BIC
462 in model selection. *Sociological Methods & Research*, *33*, 261–304.
463 doi:10.1177/0049124104268644
- 464 Caserta, F., Eldred, W. D., Fernandez, E., Hausman, R. E., Stanford, L. R., Bulderev, S. V., ...
465 Stanley, H. E. (1995). Determination of fractal dimension of physiologically characterized
466 neurons in two and three dimensions. *Journal of Neuroscience Methods*, *56*, 133–144.
467 doi:10.1016/0165-0270(94)00115-w
- 468 Chung, M. K., Nacewicz, B. M., Wang, S., Dalton, K. M., Pollak, S., & Davidson, R. J. (2008).
469 Amygdala surface modeling with weighted spherical harmonics. *Lecture Notes in*
470 *Computer Science*, *5128*, 177–184. doi:10.1007/978-3-540-79982-5_20
- 471 Chung, M. K., Worsley, K. J., Nacewicz, B. M., Dalton, K. M., & Davidson, R. J. (2010).
472 General multivariate linear modeling of surface shapes using SurfStat. *NeuroImage*, *53*,
473 491–505. doi:10.1016/j.neuroimage.2010.06.032
- 474 Creasey, H., & Rapoport, S. I. (1985). The aging human brain. *Annals of Neurology*, *17*, 2–10.
475 doi:10.1002/ana.410170103
- 476 Di Ieva, A., Esteban, F. J., Grizzi, F., Klonowski, W., & Martin-Landrove, M. (2015). Fractals in
477 the neurosciences, Part II: Clinical applications and future perspectives. *The*
478 *Neuroscientist*, *21*, 30–43. doi:10.1177/1073858413513928
- 479 Di Ieva, A., Grizzi, F., Jelinek, H., Pellionisz, A. J., & Losa, G. A. (2014). Fractals in the
480 neurosciences, Part I: General principles and basic neurosciences. *The Neuroscientist*, *20*,
481 403–417. doi:10.1177/1073858413513927
- 482 Drayer, B. P. (1988). Imaging of the aging brain. Part I. Normal findings. *Radiology*, *166*, 785–
483 796. doi:10.1148/radiology.166.3.3277247

- 484 Fischl, B., Salat, D. H., Busa, E., Albert, M., Dieterich, M., Haselgrove, C., ... Dale, A. M.
 485 (2002). Whole brain segmentation: Automated labelling of neuroanatomical structures in
 486 the human brain. *Neuron*, *33*, 341–355. doi:10.1016/s0896-6273(02)00569-x
- 487 Fischl, B., Sereno, M. I., & Dale, A. M. (1999). Cortical Surface-Based Analysis. *NeuroImage*,
 488 *9*, 195–207. doi:10.1006/nimg.1998.0396
- 489 Fjell, A. M., Westlye, L. T., Amlien, I., Espeseth, T., Reinvang, I., Raz, N., ... Walhovd, K. B.
 490 (2009). High consistency of regional cortical thinning in aging across multiple samples.
 491 *Cerebral Cortex*, *19*, 2001–2012. doi:10.1093/cercor/bhn232
- 492 Free, S. L., Sisodiya, S. M., Cook, M. J., Fish, D. R., & Shorvon, S. D. (1996). Three-
 493 dimensional fractal analysis of the white matter surface from magnetic resonance images
 494 of the human brain. *Cerebral Cortex*, *6*, 830–836. doi:10.1093/cercor/6.6.830
- 495 Goodro, M., Sameti, M., Patenaude, B., & Fein, G. (2012). Age effect on subcortical structures
 496 in healthy adults. *Psychiatry Research: Neuroimaging*, *203*, 38–45.
 497 doi:10.1016/j.psychresns.2011.09.014
- 498 Greenberg, D. L., Messer, D. F., Payne, M. E., MacFall, J. R., Provenzale, J. M., Steffens, D. C.,
 499 & Krishnan, R. R. (2008). Aging, gender, and the elderly adult brain: An examination of
 500 analytical strategies. *Neurobiology of Aging*, *29*, 290–302.
 501 doi:10.1016/j.neurobiolaging.2006.09.016
- 502 Gunning-Dixon, F. M., Head, D., McQuain, J., Acker, J. D., & Raz, N. (1998). Differential aging
 503 of the human striatum: A prospective MR imaging study. *American Journal of*
 504 *Neuroradiology*, *19*, 1501-1507.
- 505 Ha, T. H., Yoon, U., Lee, K. J., Shin, Y. W., Lee, J.-M., Kim, I. Y., ... Kwon, J. S. (2005).
 506 Fractal dimension of cerebral cortical surface in schizophrenia and obsessive–compulsive
 507 disorder. *Neuroscience Letters*, *384*, 172–176. doi:10.1016/j.neulet.2005.04.078
- 508 Hogstrom, L. J., Westlye, L. T., Walhovd, K. B., & Fjell, A. M. (2013). The structure of the
 509 cerebral cortex across adult life: Age-related patterns of surface area, thickness, and
 510 gyrification. *Cerebral Cortex*, *23*, 2521–2530. doi:10.1093/cercor/bhs231
- 511 Hrybowski, S., Aghamohammadi-Sereshki, A., Madan, C. R., Shafer, A. T., Baron, C. A., Seres,
 512 P., ... Malykhin, N. V. (2016). Amygdala subnuclei response and connectivity during
 513 emotional processing. *NeuroImage*, *133*, 98–110. doi:10.1016/j.neuroimage.2016.02.056
- 514 Im, K., Lee, J.-M., Yoon, U., Shin, Y.-W., Hong, S. B., Kim, I. Y., ... Kim, S. I. (2006). Fractal
 515 dimension in human cortical surface: Multiple regression analysis with cortical thickness,
 516 sulcal depth, and folding area. *Human Brain Mapping*, *27*, 994–1003.
 517 doi:10.1002/hbm.20238
- 518 Inano, S., Takao, H., Hayashi, N., Yoshioka, N., Mori, H., Kunimatsu, A., ... Ohtomo, K.
 519 (2012). Effects of age and gender on neuroanatomical volumes. *Journal of Magnetic*
 520 *Resonance Imaging*, *37*, 1072–1076. doi:10.1002/jmri.23910
- 521 Jernigan, T. L., Archibald, S. L., Fennema-Notestine, C., Gamst, A. C., Stout, J. C., Bonner, J.,
 522 & Hesselink, J. R. (2001). Effects of age on tissues and regions of the cerebrum and
 523 cerebellum. *Neurobiology of Aging*, *22*, 581–594. doi:10.1016/s0197-4580(01)00217-2

- 524 Kaye, J. A., DeCarli, C., Luxenberg, J. S., & Rapoport, S. I. (1992). The significance of age-
525 related enlargement of the cerebral ventricles in healthy men and women measured by
526 quantitative computed X-ray tomography. *Journal of the American Geriatrics Society*, *40*,
527 225–231. doi:10.1111/j.1532-5415.1992.tb02073.x
- 528 Keller, S. S., Gerdes, J. S., Mohammadi, S., Kellinghaus, C., Kugel, H., Deppe, K., ... Deppe,
529 M. (2012). Volume estimation of the thalamus using FreeSurfer and stereology:
530 Consistency between methods. *Neuroinformatics*, *10*, 341–350. doi:10.1007/s12021-012-
531 9147-0
- 532 Kemper T. L. (1994) Neuroanatomical and neuropathological changes during aging and
533 dementia (pp. 3–67). In: *Clinical neurology of aging, 2nd ed.* (Eds. M. L. Albert, J. E.
534 Knoefel). New York: Oxford University Press.
- 535 King, R. D., Brown, B., Hwang, M., Jeon, T., & George, A. T. (2010). Fractal dimension
536 analysis of the cortical ribbon in mild Alzheimer’s disease. *NeuroImage*, *53*, 471–479.
537 doi:10.1016/j.neuroimage.2010.06.050
- 538 King, R. D., George, A. T., Jeon, T., Hynan, L. S., Youn, T. S., Kennedy, D. N., & Dickerson, B.
539 (2009). Characterization of atrophic changes in the cerebral cortex using fractal
540 dimensional analysis. *Brain Imaging and Behavior*, *3*, 154–166. doi:10.1007/s11682-008-
541 9057-9
- 542 Kiselev, V. G., Hahn, K. R., & Auer, D. P. (2003). Is the brain cortex a fractal? *NeuroImage*, *20*,
543 1765–1774. doi:10.1016/s1053-8119(03)00380-x
- 544 La Joie, R., Fouquet, M., Mézenge, F., Landeau, B., Villain, N., Mevel, K., ... Chételat, G.
545 (2010). Differential effect of age on hippocampal subfields assessed using a new high-
546 resolution 3T MR sequence. *NeuroImage*, *53*, 506–514.
547 doi:10.1016/j.neuroimage.2010.06.024
- 548 Lehmann, M., Douiri, A., Kim, L. G., Modat, M., Chan, D., Ourselin, S., ... Fox, N. C. (2010).
549 Atrophy patterns in Alzheimer’s disease and semantic dementia: A comparison of
550 FreeSurfer and manual volumetric measurements. *NeuroImage*, *49*, 2264–2274.
551 doi:10.1016/j.neuroimage.2009.10.056
- 552 LeMay, M. (1984). Radiologic changes of the aging brain and skull. *American Journal of*
553 *Roentgenology*, *143*, 383–389. doi:10.2214/ajr.143.2.383
- 554 Long, X., Liao, W., Jiang, C., Liang, D., Qiu, B., & Zhang, L. (2012). Healthy aging. *Academic*
555 *Radiology*, *19*, 785–793. doi:10.1016/j.acra.2012.03.006
- 556 Madan, C. R. (2015). Creating 3D visualizations of MRI data: A brief guide. *F1000Research*, *4*,
557 466. doi:10.12688/f1000research.6838.1
- 558 Madan, C. R., & Kensinger, E. A. (2016). Cortical complexity as a measure of age-related brain
559 atrophy. *NeuroImage*. doi: 10.1016/j.neuroimage.2016.04.029
- 560 Mandelbrot, B. B. (1967). How long is the coast of Britain? Statistical self-similarity and
561 fractional dimension. *Science*, *156*, 636–638. doi:10.1126/science.156.3775.636
- 562 Mandelbrot, B. B. (1982). *The Fractal Geometry of Nature*. San Francisco: W.H. Freeman.
- 563 Marcus, D. S., Wang, T. H., Parker, J., Csernansky, J. G., Morris, J. C., & Buckner, R. L. (2007).
564 Open Access Series of Imaging Studies (OASIS): Cross-sectional MRI Data in young,

- 565 middle aged, nondemented, and demented older adults. *Journal of Cognitive Neuroscience*,
 566 19, 1498–1507. doi:10.1162/jocn.2007.19.9.1498
- 567 McKay, D. R., Knowles, E. E. M., Winkler, A. A. M., Sprooten, E., Kochunov, P., Olvera, R. L.,
 568 ... Glahn, D. C. (2014). Influence of age, sex and genetic factors on the human brain.
 569 *Brain Imaging and Behavior*, 8, 143–152. doi:10.1007/s11682-013-9277-5
- 570 Mulder, E. R., de Jong, R. A., Knol, D. L., van Schijndel, R. A., Cover, K. S., Visser, P. J., ...
 571 Vrenken, H. (2014). Hippocampal volume change measurement: Quantitative assessment
 572 of the reproducibility of expert manual outlining and the automated methods FreeSurfer
 573 and FIRST. *NeuroImage*, 92, 169–181. doi:10.1016/j.neuroimage.2014.01.058
- 574 Mustafa, N., Ahearn, T. S., Waiter, G. D., Murray, A. D., Whalley, L. J., & Staff, R. T. (2012).
 575 Brain structural complexity and life course cognitive change. *NeuroImage*, 61, 694–701.
 576 doi:10.1016/j.neuroimage.2012.03.088
- 577 Narr, K. L., Bilder, R. M., Kim, S., Thompson, P. M., Szeszko, P., Robinson, D., ... Toga, A. W.
 578 (2004). Abnormal gyral complexity in first-episode schizophrenia. *Biological Psychiatry*,
 579 55, 859–867. doi:10.1016/j.biopsych.2003.12.027
- 580 Nenadic, I., Yotter, R. A., Sauer, H., & Gaser, C. (2014). Cortical surface complexity in frontal
 581 and temporal areas varies across subgroups of schizophrenia. *Human Brain Mapping*, 35,
 582 1691–1699. doi:10.1002/hbm.22283
- 583 Palombo, D. J., Amaral, R. S. C., Olsen, R. K., Muller, D. J., Todd, R. M., Anderson, A. K., &
 584 Levine, B. (2013). KIBRA polymorphism is associated with individual differences in
 585 Hippocampal subregions: Evidence from anatomical segmentation using high-resolution
 586 MRI. *Journal of Neuroscience*, 33, 13088–13093. doi:10.1523/jneurosci.1406-13.2013
- 587 Pardoe, H. R., Kucharsky Hiess, R., & Kuzniecky, R. (2016). Motion and morphometry in
 588 clinical and nonclinical populations. *NeuroImage*, 135, 177–185.
 589 doi:10.1016/j.neuroimage.2016.05.005
- 590 Pienaar, R., Fischl, B., Caviness, V., Makris, N., & Grant, P. E. (2008). A methodology for
 591 analyzing Curvature in the developing brain from preterm to adult. *International Journal of*
 592 *Imaging Systems and Technology*, 18, 42–68. doi:10.1002/ima.20138
- 593 Potvin, O., Mouiha, A., Dieumegarde, L., & Duchesne, S. (2016). Normative data for subcortical
 594 regional volumes over the lifetime of the adult human brain. *NeuroImage*, 137, 9–20.
 595 doi:10.1016/j.neuroimage.2016.05.016
- 596 Qiu, A., Zhong, J., Graham, S., Chia, M. Y., & Sim, K. (2009). Combined analyses of thalamic
 597 volume, shape and white matter integrity in first-episode schizophrenia. *NeuroImage*, 47,
 598 1163–1171. doi:10.1016/j.neuroimage.2009.04.027
- 599 Raz, N., & Rodrigue, K. M. (2006). Differential aging of the brain: Patterns, cognitive correlates
 600 and modifiers. *Neuroscience & Biobehavioral Reviews*, 30, 730–748.
 601 doi:10.1016/j.neubiorev.2006.07.001
- 602 Raz, N., Lindenberger, U., Rodrigue, K. M., Kennedy, K. M., Head, D., Williamson, A., Dahle,
 603 C., Gerstorf, D., & Acker, J. D. (2005). Regional brain changes in aging healthy adults:
 604 General trends, individual differences and modifiers. *Cerebral Cortex*, 15, 1676–1689.
 605 doi:10.1093/cercor/bhi044

- 606 Raz, N., Rodrigue, K. M., Head, D., Kennedy, K. M., & Acker, J. D. (2004). Differential aging
607 of the medial temporal lobe: A study of a five-year change. *Neurology*, *62*, 433–438.
608 doi:10.1212/01.wnl.0000106466.09835.46
- 609 Reagh, Z. M., & Yassa, M. A. (2014). Object and spatial mnemonic interference differentially
610 engage lateral and medial entorhinal cortex in humans. *Proceedings of the National
611 Academy of Science USA*, *111*, E4264–E4273. doi:10.1073/pnas.1411250111
- 612 Reuter, M., Wolter, F.-E., & Peinecke, N. (2006). Laplace–Beltrami spectra as “Shape-DNA” of
613 surfaces and solids. *Computer-Aided Design*, *38*, 342–366. doi:10.1016/j.cad.2005.10.011
- 614 Salat, D. H., Buckner, R. L., Snyder, A. Z., Greve, D. N., Desikan, R. S. R., ... Fischl, B. (2004).
615 Thinning of the cerebral cortex in aging. *Cerebral Cortex*, *14*, 721–730.
616 doi:10.1093/cercor/bhh032
- 617 Sandu, A.-L., Rasmussen, I.-A., Lundervold, A., Kreuder, F., Neckelmann, G., Hugdahl, K., &
618 Specht, K. (2008). Fractal dimension analysis of MR images reveals grey matter structure
619 irregularities in schizophrenia. *Computerized Medical Imaging and Graphics*, *32*, 150–
620 158. doi:10.1016/j.compmedimag.2007.10.005
- 621 Sandu, A.-L., Staff, R. T., McNeil, C. J., Mustafa, N., Ahearn, T., Whalley, L. J., & Murray, A.
622 D. (2014). Structural brain complexity and cognitive decline in late life: A longitudinal
623 study in the Aberdeen 1936 Birth Cohort. *NeuroImage*, *100*, 558–563.
624 doi:10.1016/j.neuroimage.2014.06.054
- 625 Sargolzaei, S., Sargolzaei, A., Cabrerizo, M., Chen, G., Goryawala, M., Pinzon-Ardila, A., ...
626 Adjouadi, M. (2015). Estimating intracranial volume in brain research: An evaluation of
627 methods. *Neuroinformatics*, *13*, 427–441. doi:10.1007/s12021-015-9266-5
- 628 Seo, S., & Chung, M. K. (2011). Laplace-Beltrami eigenfunction expansion of cortical
629 manifolds. *IEEE International Symposium on Biomedical Imaging*, *2011*, 372–375.
630 doi:10.1109/isbi.2011.5872426
- 631 Smith, M. J., Wang, L., Cronenwett, W., Goldman, M. B., Mamah, D., Barch, D. M., &
632 Csernansky, J. G. (2011). Alcohol use disorders contribute to hippocampal and subcortical
633 shape differences in schizophrenia. *Schizophrenia Research*, *131*, 174–183.
634 doi:10.1016/j.schres.2011.05.014
- 635 Tae, W. S., Kim, S. S., Lee, K. U., Nam, E.-C., & Kim, K. W. (2008). Validation of hippocampal
636 volumes measured using a manual method and two automated methods (FreeSurfer and
637 IBASPM) in chronic major depressive disorder. *Neuroradiology*, *50*, 569–581.
638 doi:10.1007/s00234-008-0383-9
- 639 Tamnes, C. K., Walhovd, K. B., Dale, A. M., Østby, Y., Grydeland, H., Richardson, G., ... Fjell,
640 A. M. (2013). Brain development and aging: Overlapping and unique patterns of change.
641 *NeuroImage*, *68*, 63–74. doi:10.1016/j.neuroimage.2012.11.039
- 642 Tang, Y.-Y., Hölzel, B. K., & Posner, M. I. (2015). The neuroscience of mindfulness meditation.
643 *Nature Reviews Neuroscience*, *16*, 213–225. doi:10.1038/nrn3916
- 644 Thompson, P. M., Schwartz, C., Lin, R. T., Khan, A. A., & Toga, A. W. (1996). Three-
645 dimensional statistical analysis of sulcal variability in the human brain. *Journal of
646 Neuroscience*, *16*, 4261–4274.

- 647 Thompson, P., Moussai, J., Zohoori, A., Khan, A. A., Mega, M. S., Cummings, J. L., & Toga, A.
648 W. (1998). Cortical variability and asymmetry in normal aging and Alzheimer's disease.
649 *Cerebral Cortex*, *8*, 492–509. doi:10.1093/cercor/8.6.492
- 650 Toro, R., Poline, J.-B., Huguet, G., Loth, E., Frouin, V., Banaschewski, T., ... Bourgeron, T.
651 (2014). Genomic architecture of human neuroanatomical diversity. *Molecular Psychiatry*,
652 *20*, 1011–1016. doi:10.1038/mp.2014.99
- 653 van der Kouwe, A. J. W., Benner, T., Salat, D. H., & Fischl, B. (2008). Brain morphometry with
654 multiecho MPRAGE. *NeuroImage*, *40*, 559–569. doi:10.1016/j.neuroimage.2007.12.025
- 655 Wachinger, C., Golland, P., Kremen, W., Fischl, B., & Reuter, M. (2015). BrainPrint: A
656 discriminative characterization of brain morphology. *NeuroImage*, *109*, 232–248.
657 doi:10.1016/j.neuroimage.2015.01.032
- 658 Walhovd, K. B., Fjell, A. M., Reinvang, I., Lundervold, A., Dale, A. M., Eilertsen, D. E., ...
659 Fischl, B. (2005). Effects of age on volumes of cortex, white matter and subcortical
660 structures. *Neurobiology of Aging*, *26*, 1261–1270.
661 doi:10.1016/j.neurobiolaging.2005.05.020
- 662 Walhovd, K. B., Westlye, L. T., Amlie, I., Espeseth, T., Reinvang, I., Raz, N., ... Fjell, A. M.
663 (2011). Consistent neuroanatomical age-related volume differences across multiple
664 samples. *Neurobiology of Aging*, *32*, 916–932. doi:10.1016/j.neurobiolaging.2009.05.013
- 665 Wenger, E., Mårtensson, J., Noack, H., Bodammer, N. C., Kühn, S., Schaefer, S., ... Lövdén, M.
666 (2014). Comparing manual and automatic segmentation of hippocampal volumes:
667 Reliability and validity issues in younger and older brains. *Human Brain Mapping*, *35*,
668 4236–4248. doi:10.1002/hbm.22473
- 669 Wonderlick, J. S., Ziegler, D. A., Hosseini-Varnamkhandi, P., Locascio, J., J. Bakkour, A., van
670 der Kouwe, A., ... Dickerson, B. C. (2009). Reliability of MRI-derived cortical and
671 subcortical morphometric measures: Effects of pulse sequence, voxel geometry, and
672 parallel imaging. *NeuroImage*, *44*, 1324–1333. doi:10.1016/j.neuroimage.2008.10.037
- 673 Yang, Z., Wen, W., Jiang, J., Crawford, J. D., Reppermund, S., Levitan, C., ... Sachdev, P. S.
674 (2016). Age-associated differences on structural brain MRI in nondemented individuals
675 from 71 to 103 years. *Neurobiology of Aging*, *40*, 86–97.
676 doi:10.1016/j.neurobiolaging.2016.01.006
- 677 Yotter, R. A., Nenadic, I., Ziegler, G., Thompson, P. M., & Gaser, C. (2011). Local cortical
678 surface complexity maps from spherical harmonic reconstructions. *NeuroImage*, *56*, 961–
679 973. doi:10.1016/j.neuroimage.2011.02.007
- 680 Yun, H. J., Im, K., Jin-Ju Yang, Yoon, U., & Lee, J.-M. (2013). Automated sulcal depth
681 measurement on cortical surface reflecting geometrical properties of sulci. *PLOS ONE*, *8*,
682 e55977. doi:10.1371/journal.pone.0055977
- 683 Yushkevich, P. A., Pluta, J. B., Wang, H., Xie, L., Ding, S.-L., Gertje, E. C., ... Wolk, D. A.
684 (2015). Automated volumetry and regional thickness analysis of hippocampal subfields
685 and medial temporal cortical structures in mild cognitive impairment. *Human Brain*
686 *Mapping*, *36*, 258–287. doi:10.1002/hbm.22627

687 Zhao, G., Denisova, K., Sehatpour, P., Long, J., Gui, W., Qiao, J., ... Wang, Z. (2016). Fractal
688 dimension analysis of subcortical gray matter structures in Schizophrenia. *PLOS ONE*, *11*,
689 e0155415. doi:10.1371/journal.pone.0155415